Proceedings of the 10th World Congress on New Technologies (NewTech'24)
Barcelona, Spain - August 25-27, 2024
Paper No. ICCEIA 140
DOI: 10.11159/icceia24.140

Development of a New Laboratory Earthquake Setup Featuring a Paraffin oil-based Gel as Analogue Material

Abdallah Aoude[1], Ioannis Stefanou[1], Jean-François Semblat[2], and Vito Rubino[1]
[1]Nantes Université, Ecole Centrale Nantes, CNRS, Institut de Recherche en Génie Civil et Mécanique (GeM) UMR 6183, F-44000 Nantes, France
abdallah.aoude@ec-nantes.fr, ioannis.stefanou@ec-nantes.fr, vito.rubino@ec-nantes.fr
[2]IMSIA (UMR9219), CNRS, EDF, CEA, ENSTA Paris, Institut Polytechnique de Paris, Palaiseau 91120, Paris, France.
jean-francois.semblat@ensta-paris.fr,

Abstract **-** In this study, we present the development of a new experimental setup composed of an analogue fault surrounded by paraffin oil-based gel, which allows us to simulate earthquake-like events in the laboratory. The apparatus is designed to test the possibility of mitigating earthquake-like instabilities using control theory. We present the physical properties of the paraffin oil-based gel as functions of strain rate, strain, and temperature. Our results show a linear relation between the stress and strain up to 30% shear strain, along with a low viscosity at high strain rate. Furthermore, we engineered the frictional properties of the analogue fault using 3D-printed patches placed along its surface. Finally, an experimental earthquake simulation, using the setup, demonstrates a sudden slip event within the gel, propagating at a speed between c_s and $\sqrt{2}\,c_s$, where c_s represents the shear wave velocity of the gel, which is consistent with theoretical and previous experimental results.

Keywords**:** laboratory earthquake, paraffin oil-base gel, mechanical properties, slip propagation.

1. Introduction

Human activities can induce seismicity by injecting fluids into the Earth's crust, as observed in geothermal operations [1]. Recently, it has been demonstrated that modulating the fluid injection pressure using the mathematical theory of control is an effective strategy to mitigate earthquakes [2-5]. In this study, we present a new experimental setup designed to test the mathematical theory of control. It consists of an analogue fault surrounded by an elastic material, enabling us to study slip propagation.

Analogue materials are often employed to scale down length and time parameters by several orders of magnitude to represent conditions of the earth's crust in the laboratory. This reduction in scale enables us to monitor experimental results more effectively and compare them with real-scale scenarios using appropriate scaling laws [6-8]. Various materials have been used as analogues to the earth's crust, including foam [9,10], visco-elastic gel [11,12], rubber [13,14], and polymers such as Homalite-100 [15,16] and PMMA [17,18]. In this work, we selected paraffin oil-based gel as our analogue material for the Earth's crust due to its low elasticity, enabling us to scale down the characteristic time of the experiment. Additionally, we characterized its mechanical properties.

2. New experimental setup featuring a wedge with paraffin oil-based gel

The experimental setup includes the gel contained within a mechanical apparatus, as depicted in Fig. 1. The mechanical apparatus consists of pin connected beams, two sliders that glide along the beams, and a top plate that is pin-connected to the sliders. The left beam is fixed to the support. The frictional interface between the gel and the top plate represents the

analogue fault, with the gel representing the surrounding rocks. The components of the mechanical apparatus are 3D printed using ABS material.

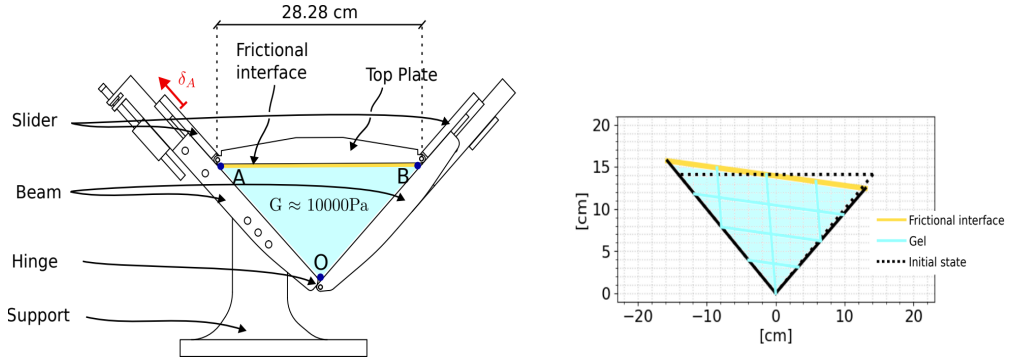

Fig. 1: Left: Gel contained within the mechanical apparatus. Right: *S*ketch showing the deformation of the gel that results by moving the left slider by δ_A.

Assuming the gel is incompressible, the system possesses only one degree of freedom. This degree of freedom is chosen to be the position of point A. Thus, by moving the left slider by an amount δ_A, the material is subjected to a unique prescribed deformation as illustrated in Fig. 1.

The interface separates two materials with significant difference in elastic properties. Such mismatch in the elastic properties profoundly influences rupture propagation. In a bimaterial interface, rupture can propagate bilaterally. The positive (negative) direction is defined as the direction where the stiffer material is in tension (compression). It has been theoretically demonstrated [19] and experimentally observed [11] that a rupture, propagating in the positive direction of a biomaterial interface with a significant mismatch in elastic properties, lies between the rupture wave speed of the soft material c_s and $\sqrt{2}\,c_s$. The rupture wave speed c_s is expressed as:

$$c_s = \sqrt{G/\rho}, \tag{1}$$

where ρ is the density of the gel and G its shear modulus.

To determine the expected range of rupture velocity, knowledge of the shear modulus of the materials is needed. In the following section, we will present the mechanical properties of the gel used in the experimental setup.

3. Mechanical properties of the paraffin oil-based gel

3.1. Theoretical Background

In this section, we present a theoretical framework to understand the rheological behaviour of the paraffin oil-based gel, which was purchased from Candelis (density = 850 kg/m^3), as well as the principles underlying experiments conducted with a rheometer.

Gels usually exhibit a viscoelastic response, as shown in Fig. 1. The material's characteristics are typically described using two moduli: the storage modulus G' (related to elasticity) and the loss modulus G'' (related to viscosity), as further elaborated below. Various tests can be conducted to study the rheology of a viscoelastic material. In this study, we employ a rheometer, utilizing parallel plates where the gel is sandwiched between them. While the bottom plate remains stationary, the upper plate oscillates at controlled frequencies (see Fig. 2). Dynamic oscillatory tests are conducted to investigate the effects of strain amplitude, strain rate, and temperature on the material.

Angular displacement is applied, and torque is measured to determine strain, strain rate, and shear stress. This enables the derivation of storage and loss moduli of the material. Let s represent the linear displacement at the edge of the sample

due to its rotation, with the sample edge located at radial distance R, as illustrated in Fig. 2. A sinusoidal displacement s is applied, expressed as:

$$\mathrm{s} = \gamma^0 sin(\omega t) y, \tag{2}$$

where γ^0 is the amplitude of strain, ω is the angular frequency, t is the time, and y is the depth of the sample (see Fig. 2). Consequently, the strain γ^{edge} at the edge of the sample is given by:

$$\gamma^{edge} = \gamma^0 sin(\omega t) y. \tag{3}$$

Similarly, the shear stress τ^{edge} at the edge is determined by:

$$\tau^{edge} = \tau^0 sin(\omega t + \delta). \tag{4}$$

Here, τ^0 is the amplitude of the shear stress, and δ is the phase shift, which arises due to the delay in response attributed to the viscosity of the material. If $\delta = 0$, the material's behavior can be described using Hooke's Law; however, if $\delta = \pi/2$, the material's behavior can be represented using Newton's Law of viscosity. For $0 < \delta < \pi/2$, the material's response can be characterized using the two moduli, G' and G'', and Eq. 4 can be rewritten as follows:

$$\tau^{edge} = G'\gamma^0 sin(\omega t) + G''\gamma^0 cos(\omega t). \tag{5}$$

Furthermore, we can derive the norm of the complex modulus $|G^*| = \tau^0/\gamma^0$, with $G' = |G^*| \cos(\delta)$ and $G'' = |G^*| \sin(\delta)$.

If we consider the Kelvin-Voigt model, when a sinusoidal oscillatory force is applied, the stress τ can be expressed as:

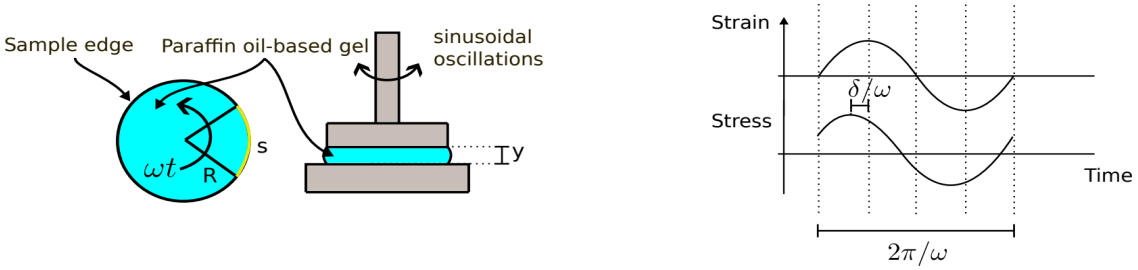

Fig. 2: Left: Sketch showing the gel sandwiched between the plates of the rheometer and exposed to oscillatory motion, along with a cross-section of the sample. Right: Strain in function of time developed at the edge of the sample and corresponding stress with phase shift due to the viscosity of the material.

$$\tau = \tau^0 sin(\omega t + \delta) = G\gamma + \eta\dot{\gamma}, \tag{6}$$

where G represents the shear modulus, η represents the dynamic viscosity, γ the shear strain, and $\dot{\gamma}$ the shear strain rate. By substituting $\gamma = \gamma^0 sin(\omega t)$ and $\dot{\gamma} = \gamma^0 \omega cos(\omega t)$ we obtain:

$$\tau = G\gamma^0 sin(\omega t) + \gamma^0 \eta\omega cos(\omega t). \tag{7}$$

By direct comparison to equation 5, we find $G = G'$ and $\omega = G''$.

3.1. Results

Three different tests are performed. The first test involved varying the strain amplitude γ^0 from 10^{-3}% to 300% while keeping the angular frequency constant at ten rad/s and the temperature at 20ºC. In the second test, the strain amplitude was kept constant at 20%, the temperature equal to 20ºC, and the frequency varied from 1 rad/s to 25 rad/s. Finally, in the third test, the temperature ranged from 9ºC to 45ºC, with the strain amplitude fixed at 20% and angular frequency at ten rad/s. The data are sampled at 3-second intervals.

In Fig. 3(a), a linear relationship between stress and strain is observed within the 10^{-3}% to 30% strain range. The ratio of stress to strain yields the norm of the complex modulus $|G^*| = \tau^0/\gamma^0$ (Fig. 3 (b)). By employing Eq. 5, we obtain G' and G''. The stress at an angular frequency of 10 rad/s and a temperature of 20ºC is given by:

$$\tau = (9992.28 \pm 48.15)\gamma + (712.02 \pm 33.75)\dot{\gamma}. \tag{8}$$

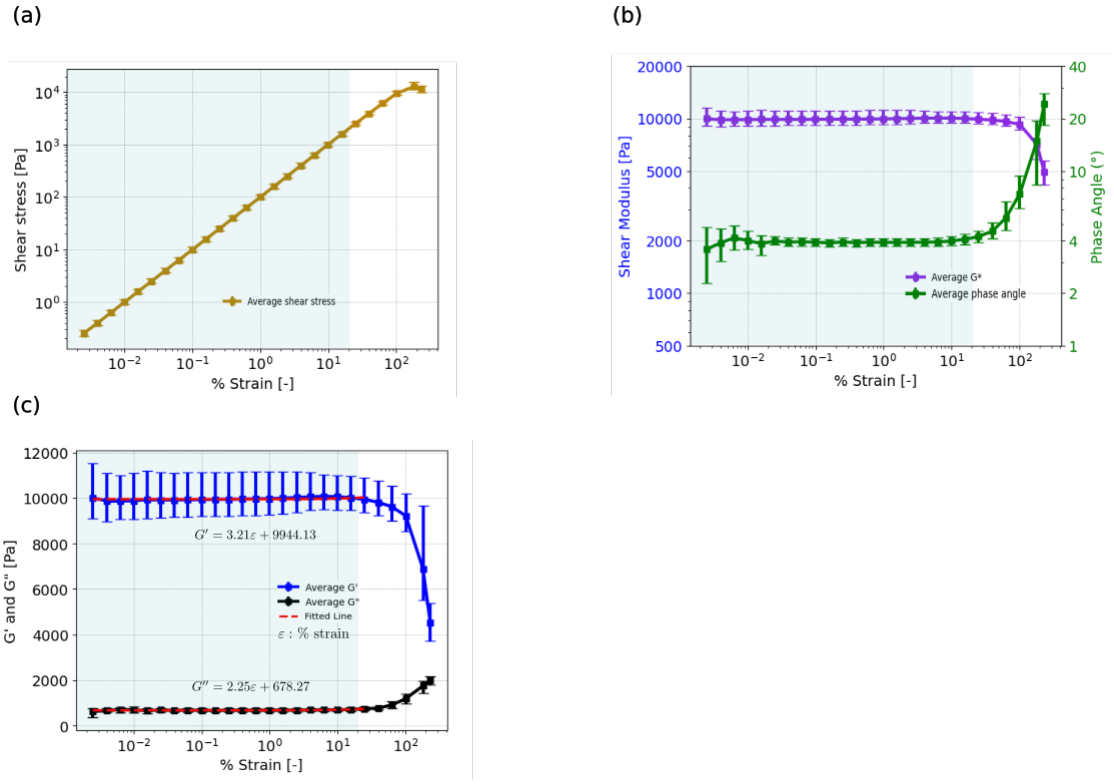

Fig. 3: a) Stress as a function of strain, b) norm of the complex modulus and phase angle as a function of strain, and c) both storage and loss moduli as functions of strain. The shaded blue area indicates the range of interest for the laboratory earthquake experiment. Error bars represent the minimum and maximum values of the readings, with values averaged from five measurements.

Regarding the sensitivity to angular frequency, the results show a tendency for the storage modulus to increase slowly, with the logarithm of the frequency, while the viscosity is inversely proportional to the frequency (see Fig. 4(a)).

The mechanical properties are sensitive to temperature, with a linear increase in G'' with temperature and an inverse cubic relationship in G' with temperature (see Fig. 4(b)). The shear stress at 10 rad/s, for 20% strain amplitude, with temperature varying from 9ºC to 45º, can be described by the following interpolation:

$$\tau = (-0.07T^{-3} + 11402.37)\gamma^0\gamma + (41.4T + 36)\gamma^0\dot{\gamma}, \tag{9}$$

where T is the temperature of the material.

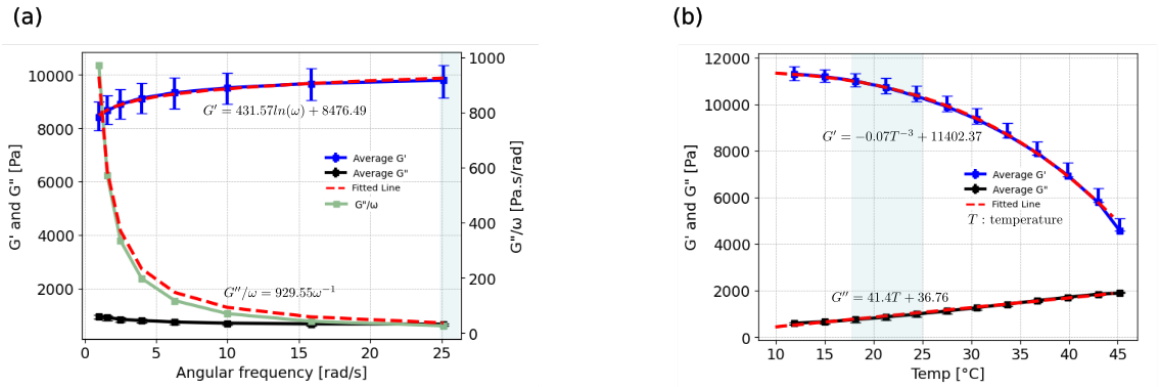

Fig. 4: a) Average of five readings of storage and loss moduli as functions of angular frequency, and b) average of three readings of storage and loss moduli as functions of temperature. The shaded blue area indicates the range of interest for the laboratory earthquake experiment. Error bars represent the minimum and maximum values of the readings.

4. Slip propagation experiment using the gel

The elastic energy in the gel as well as the shear stress at the frictional interface will increase due to the displacement of the slider by δ_A until reaching a threshold where the frictional resistance in the analogue fault is overcome, initiating sliding between the gel and the top plate. The motion is either stable or unstable. Unstable sliding occurs if the frictional force F^τ at the fault falls faster than the elastic force from the gel such as:

$$\partial F^\tau / \partial \delta < k, \tag{10}$$

where δ is the slip distance between the gel and the top plate and $k = \alpha G/L$ represents the stiffness of the gel, L is the length of the fault, G is the shear modulus of the gel, and α is a constant of the order of unity [2].

The profile of the frictional interface was designed in order to meet the instability condition. Assuming Coulomb's Law, the friction coefficient (μ) of an asperity is expressed as:

$$\mu = F^\tau / \mathrm{F}^N = tan(\Phi_b + i), \tag{11}$$

where i the inclination along the interface, Φ_b the basic friction angle, and F^N the normal force to the interface [20]. The basic friction angle is determined by the material properties and is derived from the friction coefficient of a smooth surface, as illustrated in Fig. 5.

The designed profile for the experiment is shown in Fig. 6. The total length of the asperity measures 4mm, with a height of 0.6mm. The profile was 3D printed using ABS material, with a basic friction angle of 21.8 degrees. Using Eq. 12, we calculated the corresponding friction coefficient, which is plotted in Fig. 6. The friction coefficient starts at 1 and then decreases suddenly to 0.2. With this profile, the condition of instability referred in Eq. 10 is met, as evidenced by the abrupt change in stress.

The frictional interface is discretized into 16 patches, with each patch containing the profile as presented in Fig. 7. Images are taken at 240 fps to measure the slip propagation, and then the position of the patches is tracked using the com-

mercial software Tema by Image Systems Motion Analysis, Inc. In the experiment, the slip started from the left and propagated to the right, as shown in Fig. 8. The slip propagated 5.48 cm in 3/240 seconds. This gives an average rupture speed of 4.4m/s.

To determine the mechanical properties during slip propagation, we utilize the relationship between linear velocity (v) and angular frequency (ω), expressed as $v = R\omega$, where R is the radius of the sample used to characterize the gel (see Fig. 2). With a linear velocity of 4.4m/s, the corresponding angular frequency is calculated as 220rad/s. At this angular frequency, the storage modulus is 10804 Pa, and the dynamic viscosity is 4.2 Pa.s/rad (see Fig. 4(a)). Therefore, we can consider that viscous effects are secondary during the slip. The measure average rupture speed in the positive direction is between c_s and $\sqrt{2}\,c_s$, where $c_s = \sqrt{G/\rho} = 3.4$ m/s, consistent with theoretical results [19] and experimental observations [11].

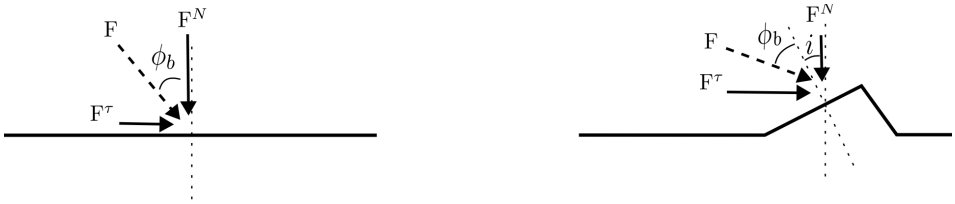

$$\mu = \frac{F^\tau}{F^N} = tan(\Phi_b) \qquad \mu = \frac{F^\tau}{F^N} = tan(\Phi_b + i)$$

Fig. 5: Left: Frictional interface with a smooth surface. Right: Frictional interface with asperity inclination.

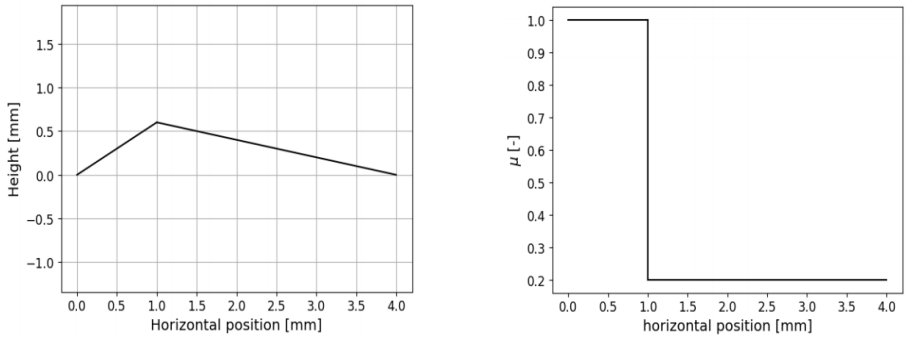

Fig. 7: Left: Profile of the designed asperity as function of horizontal position. Right: Friction coefficient as function of horizontal position.

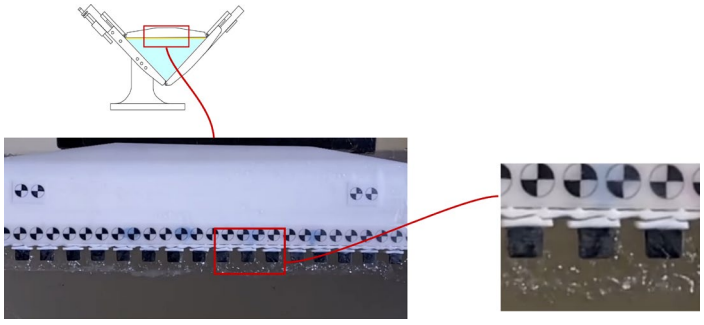

Fig. 6: Image showing the printed asperities along the frictional interface.

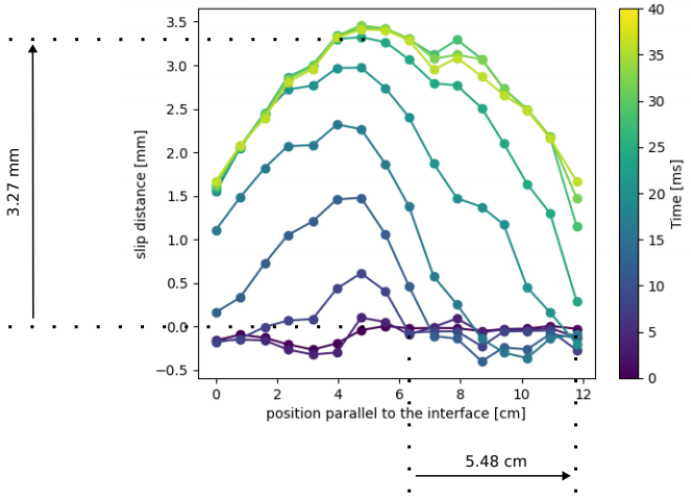

Fig. 8: Slip profile along a section on the frictional interface acquired at 240 fps.

5. Conclusion

In this study, we have presented a new laboratory earthquake setup composed of an interface with specified roughness surrounded by paraffin oil-based gel in the bulk. The soft gel was chosen to reduce the characteristic time of dynamic instabilities. The interface was engineered to meet the condition of instability, thereby simulating earthquake-like events in the laboratory. We experimentally characterized the mechanical properties of paraffin oil-based gel. The tests performed showed a linear relation between the stress and strain for strain amplitude between 10^{-3}% and 30%, with storage modulus G' =9992.28±48.15Pa and G''= 712.02±33.75Pa, at 20ºC and ω=10 rad/s. The storage modulus increases logarithmically with the angular frequency, but is inversely cubic with temperature. The viscous term is inversely proportional to the angular frequency, but increases linearly with temperature. To demonstrate the capabilities of the setup, an experiment was performed using the apparatus to simulate an earthquake, and the rupture propagation speed was measured using particle tracking velocimetry. The rupture propagates at a speed between the rupture wave speed of the soft material c_s and $\sqrt{2}\,c_s$ in the positive direction, as expected, based on previous theoretical estimates and experimental observations. Viscosity effects were found to be secondary during an instability. In future work, the effective stress will be modulated over the analogue fault using the control theory [2-5] to mitigate instabilities and achieve controlled slip rates.

References

[1] Majer, E. L., Baria, R., Stark, M., Oates, S., Bommer, J., Smith, B., & Asanuma, H. (2007). Induced seismicity associated with enhanced geothermal systems., *Geothermics,* vol. 36, no. 3, pp. 185-222, 2007.

[2] Stefanou, I. (2019). Controlling anthropogenic and natural seismicity: Insights from active stabilization of the spring-slider model. *Journal of Geophysical Research: Solid Earth*, *124*(8), 8786-8802.

[3] Stefanou, I., & Tzortzopoulos, G. (2022). Preventing instabilities and inducing controlled, slow-slip in frictionally unstable systems. *Journal of Geophysical Research: Solid Earth*, *127*(7), e2021JB023410.

[4] Tzortzopoulos, G. (2021). *Controlling earthQuakes (CoQuake) in the laboratory using pertinent fault stimulating techniques* (Doctoral dissertation, École centrale de Nantes).

[5] Gutiérrez-Oribio, D., Tzortzopoulos, G., Stefanou, I., & Plestan, F. (2023). Earthquake control: An emerging application for robust control. theory and experimental tests. *IEEE Transactions on Control Systems Technology*.

[6] Rosenau, M., Lohrmann, J., & Oncken, O. (2009). Shocks in a box: An analogue model of subduction earthquake cycles with application to seismotectonic forearc evolution. *Journal of Geophysical Research: Solid Earth*, *114*(B1).

[7] Rosenau, M., Corbi, F., & Dominguez, S. (2017). Analogue earthquakes and seismic cycles: Experimental modelling across timescales. *Solid Earth*, *8*(3), 597-635.
[8] Caniven, Y., Dominguez, S., Soliva, R., Cattin, R., Peyret, M., Marchandon, M., Romano, C., & Strak, V. (2015). A new multilayered visco-elasto-plastic experimental model to study strike-slip fault seismic cycle. *Tectonics*, *34*(2), 232-264.
[9] Brune, J. N., Brown, S., & Johnson, P. A. (1993). Rupture mechanism and interface separation in foam rubber models of earthquakes: A possible solution to the heat flow paradox and the paradox of large overthrusts. *Tectonophysics*, *218*(1-3), 59-67.
[10] Anooshehpoor, A., & Brune, J. N. (1994). Frictional heat generation and seismic radiation in a foam rubber model of earthquakes. *pure and applied geophysics*, *142*, 735-747.
[11] Latour, S., Gallot, T., Catheline, S., Voisin, C., Renard, F., Larose, E., & Campillo, M. (2011). Ultrafast ultrasonic imaging of dynamic sliding friction in soft solids: The slow slip and the super-shear regimes. *Europhysics Letters*, *96*(5), 59003.
[12] Namiki, A., Yamaguchi, T., Sumita, I., Suzuki, T., & Ide, S. (2014). Earthquake model experiments in a viscoelastic fluid: a scaling of decreasing magnitudes of earthquakes with depth. *Journal of Geophysical Research: Solid Earth*, *119*(4), 3169-3181.
[13] Hamilton, T., & McCloskey, J. (1997). Breakdown in power-law scaling in an analogue model of earthquake rupture and stick-slip. *Geophysical research letters*, *24*(4), 465-468.
[14] Hamilton, T. O. N. Y., & McCloskey, J. O. H. N. (1998). The predictability of large earthquakes: Evidence from an analogue model of earthquake rupture. *pure and applied geophysics*, *152*, 23-35.
[15] Rubino, V., Rosakis, A. J., & Lapusta, N. (2017). Understanding dynamic friction through spontaneously evolving laboratory earthquakes. *Nature communications*, *8*(1), 15991.
[16] Tal, Y., Rubino, V., Rosakis, A. J., & Lapusta, N. (2020). Illuminating the physics of dynamic friction through laboratory earthquakes on thrust faults. *Proceedings of the National Academy of Sciences*, *117*(35), 21095-21100.
[17] Gori, M., Rubino, V., Rosakis, A. J., & Lapusta, N. (2021). Dynamic rupture initiation and propagation in a fluid-injection laboratory setup with diagnostics across multiple temporal scales. *Proceedings of the National Academy of Sciences*, *118*(51), e2023433118.
[18] Paglialunga, F., Passelègue, F., Lebihain, M., & Violay, M. (2024). Frictional weakening leads to unconventional singularities during dynamic rupture propagation. *Earth and Planetary Science Letters*, *626*, 118550.
[19] Huang, Y., Wang, W., Liu, C., & Rosakis, A. J. (1998). Intersonic crack growth in bimaterial interfaces: an investigation of crack face contact. *Journal of the Mechanics and Physics of Solids*, *46*(11), 2233-2259.
[20] Braun, P., Tzortzopoulos, G., & Stefanou, I. (2021). Design of Sand-Based, 3-D-Printed Analog Faults With Controlled Frictional Properties. *Journal of Geophysical Research: Solid Earth*, *126*(5), e2020JB020520.